Enhanced Equivalent Model Algorithm for Solar Mirrors

Marco Montecchi[1,a)], Florian Sutter[2], Aránzazu Fernández-García[3], Anna Heimsath[4], Francisco Torres[4] and Cristina Pelayo[5]

[1]*ENEA C.R. Casaccia, Department of Energy Technologies, Via Anguillarese, 301, 00123 S. Maria di Galeria, Roma, Italy*
[2]*DLR, Institute of Solar Research, Plataforma Solar de Almería, Senes Road, Km. 4.5, P.O. Box 44, E04200 Tabernas, Almería, Spain*
[3]*CIEMAT-Plataforma Solar de Almería, Senes Road, Km. 4.5, P.O. Box 22, E04200 Tabernas, Almería, Spain*
[4]*Fraunhofer-Institut für Solare Energiesysteme ISE, Heidenhofstr. 2, 79110 Freiburg, Germany*
[5]*Universidad de Zaragoza, Department of Applied Physics, Maria de Luna 3, 50018 Zaragoza, Spain*

[a)]Corresponding author: marco.montecchi@enea.it

Abstract. The SolarPACES Reflectance Guideline provides an essential tool to obtain comparable reflectance measurements, but because of the lack of adequate commercial instrumentation, till now the exhaustive characterization of reflectance behaviour versus incidence θ_i and (half) acceptance angle φ is unachieved. An expert group in Task III has been working to outline some practicable solutions. The Equivalent Model Algorithm (EMA) was found quite promising: with few input data, EMA allows to predict any reflectance feature by computation. The recent availability of reliable reflectance measurements at oblique incidence made possible the refinement of EMA by analysing a representative set of commercial solar mirrors. This paper describes the new EMA for solar mirror, named EMA4SM, and reports its validation[1].

INTRODUCTION

In concentrating solar power (CSP) plants, mirrors are used to redirect solar radiation on a receiver [1]. Mirrors represent the first link in the energy-conversion chain from sun to thermal power or to electricity-delivery in the grid. *Shape* and *solar reflectance* are the key-parameters of solar mirrors affecting how solar radiation is concentrated around the focus, and how much of the impinging solar power is reflected, respectively.

SolarPACES is the leading international network of researchers in thermal solar for dispatchable power and solar chemistry technologies. The annual conferences represent a very important opportunity for gathering industries and scientists, each with their own vision and necessity. By now, the need of a clear definition of the parameters needed to qualify components and systems for CSP applications, as well as suitable methods to measure them, has been well established: only shared consensus on parameters and methods allows concurrent industrial products available on the market to be equitably qualified and compared.

In SolarPACES Task III, an international group of experts is drafting the guidelines. The latest Reflectance Guideline [2] is the result of a years-long debate, and benefits of three reflectance round robin tests [3, 14, 16], as well as of the SolarPACES project titled *Reflectance Measurement Working Group under SolarPACES Task III* (2014-2017) to fund two workshops. One of the most crucial points treated in the document is the evaluation of solar-weighted hemispherical reflectance. The recommended procedure consists of measuring:

- at near-normal incidence,
- with a high quality spectrophotometer
- equipped with an integrating sphere with diameter not lower than 150 mm,
- in the solar wavelength range (320-2500 nm).

[1]Based on experiments carried out at ENEA.

SolarPACES 2019
AIP Conf. Proc. 2303, 100005-1–100005-10; https://doi.org/10.1063/5.0028768
Published by AIP Publishing. 978-0-7354-4037-1/$30.00

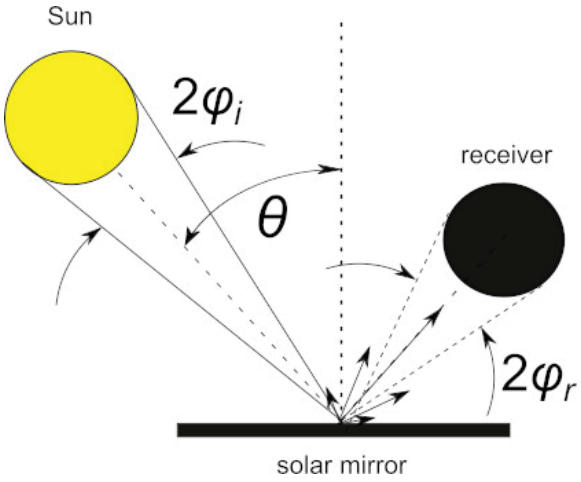

FIGURE 1. In CSP applications, mirrors generally work at off-normal incidence; reflected radiation is generally more divergent than the incident one ($2\varphi_i$) because of imperfections; the receiver collects only the radiation reflected/diffused in the acceptance angle $2\varphi_r$. For the sake of simplicity in the following φ_r will be referred as φ

- Finally, the experimental spectrum should be weighted with the Air Mass 1.5 direct normal reference solar spectrum specified in ASTM G173-03.

Unfortunately, in CSP applications the knowledge of near-normal hemispherical reflectance alone is not enough: as shown in Fig. 1, mirrors generally work at off-normal incidence, the solar radiation is a bit diverging ($\varphi_i \sim 5$ mrad), and only the radiation reflected in the acceptance-angle $2\varphi_r$ of the receiver is intercepted (for the sake of simplicity in the following φ_r will be referred as φ). Because that kind of reflectance does not coincide with either *hemispherical* and *near-specular*, the new parameter Sun Conic Reflectance[8] (SCR) has been recently proposed; it represents the amount of solar radiation reflected by the mirror in the acceptance angle 2φ of the receiver. SCR can be directly measured by setting the divergence of the light measurement beam to the typical value of the solar radiation on the earth (about 5 mrad of half-angle) and arranging the detector unit to collect only the radiation contained in a well defined acceptance angle.

The importance of also measuring near-specular / sun-conic reflectance is now fully acknowledged, so much so that SolarPACES, with the new project "Measuring and modelling near-specular solar reflectance at different incidence angles", has recently granted funds for the development/upgrading of SMQ, VLABS and S2R instruments as well as the custom spectrophotometer of Zaragoza University [16]. The project included the accomplishment of a new round robin, and aimed to give a significant improvement to the reflectance guidelines. The project is now successfully completed; the new Enhanced Equivalent Model Algorithm for Solar Mirrors (EMA4SM) is one of the most valuable achieved results. EMA4SM represents the evolute adaptation to the case of solar mirrors of the Equivalent Model Algorithm (EMA) originally proposed for modelling the angular behaviour of architectural glazing [9]; this progress has been made possible thanks to the recent availability of reliable reflectance measurements at oblique incidence.

Concerning the instruments prepared by each one of the institutions belonging to the reflectance expert group of SolarPACES Task III, the new instrument S2R [7], as well as the custom spectrophotometer arranged at the Zaragoza University [16], benefits of the new concept of sun-conic radiation, which is there directly measured at oblique incidence, in the solar range, with polarization *s* and *p*; the average (unpolarized) spectrum is solar-weighted, getting the sun conic reflectance value at the selected incidence and acceptance angle. The main drawback of these instruments is the long measuring time: the whole measurement takes 1 hour about for just a couple of values θ_i and φ.

In order to make the experimental set-up simple, the other two partners F-ISE and ENEA followed a different way, by developing respectively the innovative instruments VLABS [6] and SMQ2 [4] for measuring the near-specular reflectance in a range of acceptance angle at one selected single-wavelength, and incidence angle θ_i. The measurement is quite fast because based on image processing. Measurements are repeated at three different wavelengths (blue, green, and red) and the results are properly modelled in order to extend the evaluation in the solar range.

More precisely: the procedure adopted by F-ISE requires measurements at oblique incidence θ_i of both hemispherical (in the solar range) and near-specular reflectance (with VLABS); these data are processed by means of the

Total Integrated Scattering equation (TIS) [12] and the predictions are limited to the considered incidence angle θ_i.

The ENEA approach is more ambitious: in SMQ2 the incidence angle is always set at $\theta_i = 3°$, and prediction over the whole solar wavelength range [320,2500] nm, as well as incidence [0,90] deg and acceptance [0-50] mrad angular range is ensured by an accurate optical model of which the new EMA for solar mirror, named EMA4SM, represents the latest evolution.

Currently EMA4SM allows to predict the solar-weighted reflectance behaviour versus incidence and acceptance angle behaviour from few experimental data measured at near normal incidence, such as: 1) hemispherical reflectance spectrum measured in the solar range [320, 2500] nm; 2) near-specular or conic reflectance measured at single wavelength and several different acceptance angles in the range of interest.

This paper describes EMA4SM, and reports its validation on a specimen-set representative of the commercial production; more precisely the results achieved with SMQ2 were used as entry data of EMA4SM, and the obtained predictions were compared with the experimental results got by the other instruments developed in the project.

THEORY OF EMA4SM

EMA was proposed about twenty years ago to predict angular-properties of architectural-glazing [9]: daylighting and energy consumption evaluation for actual rooms requires knowledge of the luminous and energetic parameters of the fenestration, also at off-normal incidence. In spite of that, international standards recognize only near-normal incidence spectrophotometric measurements as reliable enough to be adopted [10]. The exhaustive optical characterization of the fenestration allows one to evaluate off-normal incidence behaviour, but it is quite complex in the case of multilayer coatings. For that, several simple algorithms, among them EMA, have been proposed.

EMA is based on the fact that even if totally unrealistic, optical models perfectly reproducing the experimental measurements at near-normal incidence, predict off-normal incidence features, averaged on the solar or visible spectrum, with good accuracy.

The Equivalent Model Algorithm for Solar Mirrors (EMA4SM) described in present paper represents the latest evolute adaptation of EMA to the specific case of solar mirrors with the precise final purpose to predict the angular behaviour versus incidence and acceptance angle of the solar-weighted reflectance.

EMA4SM is composed by two main parts: the optical model and the algorithm, that is the workflow. These are the subjects of the following subsections.

The Optical Model

Solar mirrors can be divided into two categories: glass-based and innovative. In the first case, the metallic layer (typically silver) is deposited on one of the two sides of a glass substrate and then protected by a special painting; the other side of the glass is used as specular surface, thus most of the solar radiation has to travel back and forth through the glass thickness before travelling towards the receiver. Generally the glass is enough thick to maintain the desired shape after the forming process; the usage of glasses with low metal content is preferable to reduce the absorption and increase the reflectance.

Innovative mirrors are characterized by using a substrate other than glass, and being a “first surface mirror”. Such new thin solar mirrors are offered as optical coatings or thin foils to be, respectively, deposited on or laminated to a rigid substrate which gives the desired shape to the facet. For economic reasons, the surface of that substrate (generally aluminium) cannot be polished to ensure high optical quality; therefore surface roughness causes a light scattering phenomenon, large enough to appreciably spread the reflected solar beam compared to conventional glass solar mirrors. However in CSP, as described in Figure 1, mirrors are just used to concentrate solar radiation on the receiver, and not for imaging the Sun: all the radiation reflected in the solid angle of receiver-viewing is useful.

From the optical point of view both typologies of solar mirrors, glass-based and innovative, are well represented by the model sketched in Figure 2: to ensure a good durability, the useful side of the metallic layer is always covered by a protective transparent layer which thickness ranges from few (glass-based) to tenths of millimetre (innovative). Although for the latter the over-layer thickness is sometimes less than the coherence length of the radiation, and some interference effects are visible in the reflectance spectrum, in the following, for the sake of simplicity, the optical system will be always considered like a not coherent double interface; in other words, the reflection terms at the two interfaces will be summed up in a not coherent manner as described in [11].

The roughness at the interface between over and metallic layers is used to model the spreading of the reflected radiation around the specular direction; its RMS value, $\sigma(\varphi_p)$, is here considered as just an heuristic parameter, and

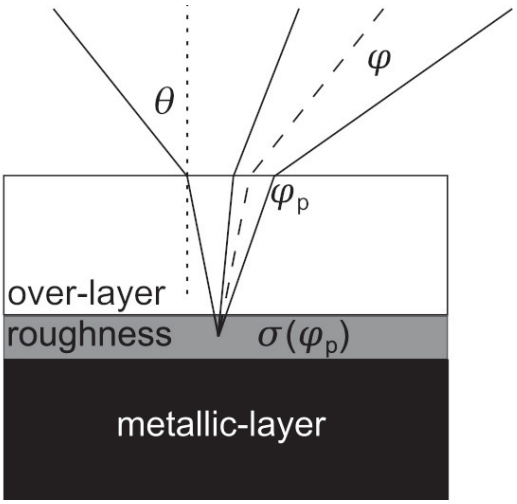

FIGURE 2. sketch of the optical model used in EMA4SM.

for that unrealistically depends on the acceptance angle internal to the over-layer φ_p, where the subscript "p" refers to the plane of incidence (the one depicted in Figure 2).

Orthogonally to the plane of incidence, along the "s" plane, the internal acceptance angle φ_s does not depend on the incidence angle.

The internal acceptance angles φ_p and φ_s, related to the acceptance angle in air φ by Snell's low, are

$$\varphi_s = \arcsin\left(\frac{\sin\varphi}{n_{ol}}\right) \approx \frac{\varphi}{n_{ol}} \tag{1}$$

$$\varphi_p = \frac{1}{2}\left[\arcsin\left(\frac{\sin(\theta_i+\varphi)}{n_{ol}}\right) - \arcsin\left(\frac{\sin(\theta_i-\varphi)}{n_{ol}}\right)\right] \approx \frac{\cos(\theta_i)}{\cos(\theta_{ol})}\frac{\varphi}{n_{ol}}. \tag{2}$$

At normal incidence $\varphi_p = \varphi_s$; but as soon as the incidence angle increases from normal incidence, $\varphi_p < \varphi_s$, giving reason of the decreasing reflectance behaviour observed for many different specimens: as matter of fact, the equivalent roughness (reflectance) generally increases (decreases) for small acceptance angles.

That is the major improvement of the new optical model with respect to the previous one proposed in [5], where the mirror scattering was simply modelled by applying the Total Integrated Scattering (TIS) equations [12] to the overall near-specular and hemispherical reflectance by the equation

$$\frac{\rho_{\lambda,\varphi}(\lambda,\theta_i,\varphi)}{\rho_{\lambda,h}(\lambda,\theta_i,h)} = \exp\left[-\left(\frac{4\pi\sigma_\varphi\cos\theta_i}{\lambda}\right)^2\right]; \tag{3}$$

unfortunately that is not completely correct because TIS refers to a metallic rough surface directly faced to the air, and its near specular reflectance is expected to increase with the incidence angle, screeching with experimental evidence.

Conversely, in EMA4SM the TIS equation just acts on the reflectance terms due to the interface over-layer || metallic-layer; as described in [11] these terms are combined with the other ones due to the air || over-layer interface by the equation

$$R_j = R_{aj} + \frac{(1-R_{aj})^2 R_{bj}\eta}{\exp(2\alpha d) - R_{aj}R_{bj}\eta} \tag{4}$$

with $j = s, p$ polarization, R_a and R_b reflectance at the interface air || over-layer ("a") and over-layer || metallic-layer ("b"), d over-layer thickness,

$$\alpha = \frac{4\pi}{\lambda}\Im\left(-\sqrt{(n_{ol}-ik_{ol})^2 - \sin(\theta_i)^2}\right) \tag{5}$$

absorption coefficient, λ wavelength in air, n_{ol} and k_{ol} refractive index and extinction coefficient of the over-layer, and η damping factor of R_b driven by the roughness: in the case of hemispherical reflectance $\eta = 1$, otherwise, in the case

of near-specular reflectance,

$$\eta = wE_s + (1 - w)(E_s + E_p)/2 \tag{6}$$

with $w = \left(\frac{\varphi_p}{\varphi_s}\right)^2$ and

$$E_s = \exp[-(4\pi\sigma(\varphi_s)\cos(\theta_{ol})n_{ol}/\lambda)^2] \tag{7}$$

$$E_p = \exp[-(4\pi\sigma(\varphi_p)\cos(\theta_{ol})n_{ol}/\lambda)^\beta] \tag{8}$$

where E_s and E_p are identical and simile like to the TIS equation actualized to the interface "b", respectively. The exponent β in E_p is used as trimmer parameter to improve the agreement of the predictions with the experimental data: at normal incidence $w = 1$, thus η =TIS; as soon as the incidence angle increases, w becomes smaller than 1, and the damping factor η can be reduced further by setting β less than 2.

We have been forced to include the trimmer parameter β, because the only reduction of φ_p as θ_i increases was found not sufficient to explain the angular behaviour experimentally observed. Unfortunately at the present we have not a physical explanation for that.

For completeness we also report the formula to calculate R_{aj} and R_{bj} [13]:

$$R_s = \left(\frac{N_1\cos(\theta_1) - N_2\cos(\theta_2)}{N_1\cos(\theta_1) + N_2\cos(\theta_2)}\right)^2 \tag{9}$$

$$R_p = \left(\frac{N_2\cos(\theta_1) - N_1\cos(\theta_2)}{N_2\cos(\theta_1) + N_1\cos(\theta_2)}\right)^2 \tag{10}$$

$$\theta_2 = \arcsin(N_1\sin(\theta_1)/N_2), \tag{11}$$

where $N_m = n_m - ik_m$, and the index "1" and "2" refer to the materials composing the interface, i.e. $N_1 \| N_2$ where the materials are air || over-layer and over-layer || metallic-layer for the interface "a" and "b", respectively.

The Algorithm

The optical model has to be adjusted to fit some experimental measurements accomplished on the specimen of interest. Concerning the over-layer thickness, in the case of glass-based mirrors, it can be measured by a calliper; otherwise, for innovative ones, it shall be arbitrary set to 0.1 mm, unless the manufacturer makes that data available.

Nowadays the near-normal hemispherical spectral reflectance is a reliable measurement [14], also thanks to the well defined procedure described in [2]; for that we consider it as the first entry data for EMA4SM, used for setting the complex refractive index of over and metallic layers.

More precisely, the complex refractive index of the metallic-layer is set to the most suitable literature value. Concerning the over-layer, in the case of glass-based mirrors, generally a bare specimen of the glass substrate is available; therefore its complex refractive index can be determined on the basis on reflectance and transmittance spectra measured at near-normal in the solar range as described in [15]. Otherwise, or in any case for innovative mirrors, the complex refractive index of the over-layer shall be set to the literature data of some simile like material.

In any case, if in the UV region the absorption across the over-layer is high enough to completely mask the reflection from the inner interface "b", the refractive index of the over-layer can be determined from the UV reflectance because it is only due to the interface "a" air || over-layer; that data are useful to choice the most proper simile like material for the over-layer.

All these data, as well as the hemispherical reflectance spectrum, shall be splined on a common set of wavelengths in the solar range. Finally, wavelength by wavelength, just one parameter of the model has to be numerically refined until the simulated hemispherical reflectance perfectly fit the experimental value. In the case of innovative mirrors, the model can be refined by means of the extinction coefficient of the over-layer; in the case of glass-based, the adjustment can be dealt via the extinction coefficient of the metallic-layer. Of course all this is quite arbitrary, but on the other hand it easy to verify the low influence of such a choice on the final results, that is the solar weighted reflectance.

The next step is the proper setting of the roughness parameter $\sigma(\varphi_{ol})$ on the basis of experimental measurements at single wavelength of near-specular or conic reflectance at several values of the acceptance angle in range of interest of the solar mirror. To make easier this task, it is convenient to express $\sigma(\varphi_{ol})$ as a suitable analytical function, such as

$$\sigma(\varphi_{ol}) = A_0 + A_1\exp\left[-\left(\frac{\varphi_{ol}}{S_1}\right)^2\right] + A_2\exp\left[-\left(\frac{\varphi_{ol}}{S_2}\right)^2\right] \tag{12}$$

where $\varphi_{ol} = \varphi_s$ or φ_p; Equation 12 was found suitably working for dozens of different solar mirror specimens. In such a way the task of setting the roughness of the model is accomplished by best fitting the experimental near-specular or conic reflectance data by means of the parameters $A_0,\ A_1,\ S_1,\ A_2,\ S_2$.

Although the optical model could be adjusted by off-normal incidence measurements of near-specular or conic reflectance at single wavelength with polarised light, measuring at near-normal incidence, without need of polarized light, is much simpler.

Once also the roughness is properly set, the optical model is ready to predict hemispherical, near-specular as well as sun conic reflectance at whatever polarization, incidence angle, and acceptance angle (but inside the investigated range).

In particular, the sun conic reflectance can be computed starting from the near-specular reflectance as described in the Appendix. Noteworthy the inverse path, i.e. the computing of near-specular from sun conic reflectance, can not be done via some formulas, but requires the optical modelling of the mirror because the reflected-beam spreading is due to two different causes, the solar radiation divergence and the mirror scattering, which effects can not be distinguished one from the other.

EXPERIMENTAL VALIDATION OF EMA4SM

ENEA prepared, and has made available to the other partners, the software SMQexpo which embeds optical model and workflow of EMA4SM. The software is written in C++ and equipped with a graphical interface based on the Qt libraries; it is designed to accept as entry data the results got with any of the other instruments.

In order to validate EMA4SM, a specimen-set representative of the commercial production have been measured with all the developed instruments. The set is composed by four solar mirrors based on: i) aluminium; ii) polymer; iii) glass with anti-soiling treatment; iv) traditional glass.

In the present paper EMA4SM is validated on the specimen-set by using the experimental measurements accomplished by ENEA as entry data, and comparing the obtained predictions with the experimental results got by the other instruments developed in the project.

The first row of Figure 3 shows the entry data: i) the hemispherical reflectance spectrum (on the left) measured in the solar range with a Perkin Elmer Lambda 1050 equipped with a 150 mm integrating sphere at $\theta_i = 8$ deg; ii) the near specular reflectance (on the right) measured with SMQ2 at 550 nm (for greater clarity the data at 480 and 650 nm have not been reported here) at $\theta_i = 3$ deg, in the acceptance-angle range [3-50] mrad. As matter of fact, the light source of SMQ2 is a collimated laser with beam divergence less than 1mrad; for this reason the measured reflectance by SMQ2 is approximately equal to the near-specular reflectance and is denominated in this way in the present paper. Finally, the obtained equivalent roughness and an exemplary output of EMA4SM are shown in the second row of Figure 3.

Figure 4 shows the comparison among the EMA4SM prediction with the experimental results got at $\theta_i = 10,\ 30,\ 60$ deg and $\varphi = 15$ mrad with S2R and UNIZA spectrophotometers and with the VLABS predictions. The best agreement was obtained by setting the trimmer parameter to $\beta = 1.3$. The uncertainty of EMA4SM prediction represents the standard deviation among the evaluations achieved at the three wavelengths 480, 550, and 650 nm. The results from one instrument to another are completely independent, apart the specimen; the typical uncertainty of the absolute reflectance is ±0.7 %, including the typical errors on reference mirror and base-line drift of the spectrophotometer. Noteworthy, the VLABS data shown in Figure 4 are near-specular values which are expected to be a bit greater than sun-conic values for less than 0.5%.

Except for ”polymer” and ”traditional” results got by UNIZA, which values seem a bit over-valuated, the agreement for all the other cases is within the uncertainty, demonstrating the validity of EMA4SM approach. The exceptions observed for UNIZA probably arise from the insufficient homogeneity of the detector area; the measurements will be repeated as soon as the instrument will be suitably upgraded.

In a next paper EMA4SM will be fed with the data got by each one of the developed instruments in order to demonstrate the independence of its predictions from the specific adopted instrument. Moreover, the comparison at more than one φ value will be shown.

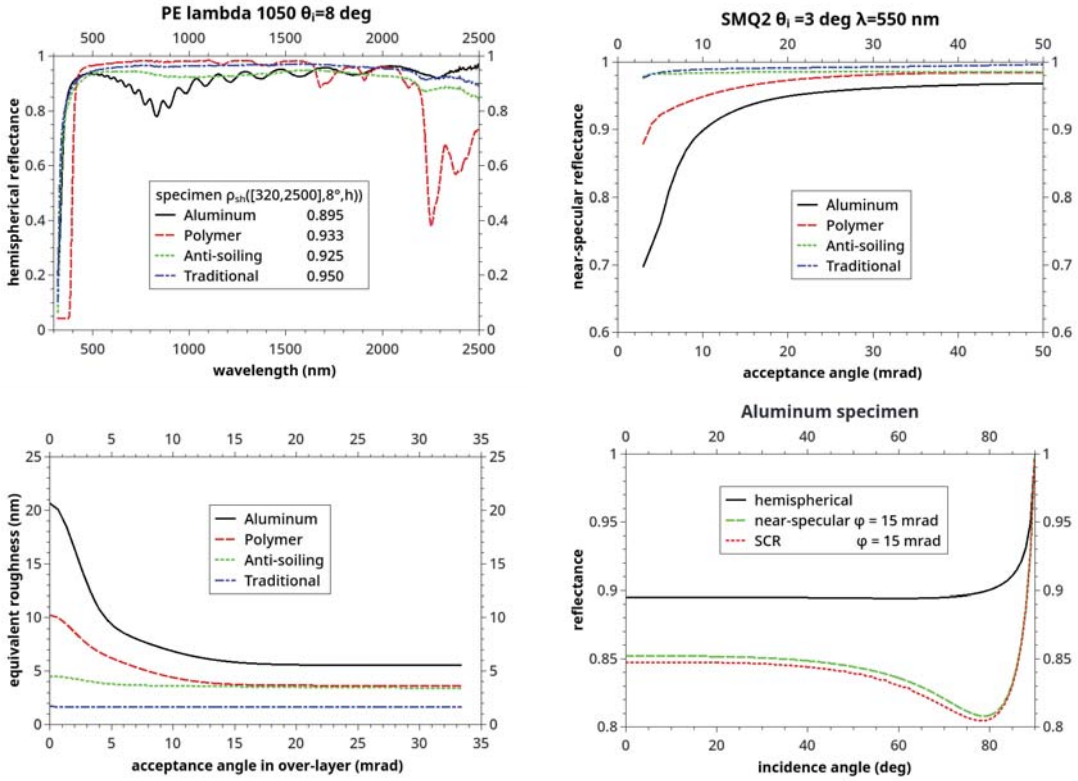

FIGURE 3. In the first row, the experimental measurements of the specimen-set used as entry data for EMA4SM: hemispherical reflectance spectrum in the solar range (left) and near-specular reflectance at single wavelength (only 550 nm is shown) in [3,50] mrad (right). In the second row, the obtained equivalent roughness (left) and an exemplary output of EMA4SM (right).

CONCLUSIONS

The Equivalent Model Algorithm for Solar Mirrors (EMA4SM) described in the present paper represents the latest evolute adaptation of EMA to the specific case of solar mirrors with the target of predicting the angular behaviour versus incidence and acceptance angle of the solar-weighted reflectance.

EMA4SM needs of few experimental data measured at near normal incidence, such as: 1) hemispherical reflectance spectrum measured in the solar range [320, 2500] nm; 2) near-specular or conic reflectance measured at single wavelength and several different acceptance angles in the range of interest.

In the paper EMA4SM has been successfully validated on a specimen-set representative of the commercial production; more precisely the results achieved with SMQ2 were used as entry data for EMA4SM, and the obtained predictions were compared with the experimental results got by the other instruments developed in the project.

Except two cases where the results by UNIZA seem a bit over-valuated, for all the other cases the agreement is within the uncertainty, demonstrating the validity of EMA4SM approach. These exceptions probably arise from the insufficient homogeneity of the detector area across the acceptance angle; after a suitably upgrading of UNIZA spectrophotometer, the measurements will be repeated.

In a next paper EMA4SM will be fed with the data got by each one of the developed instruments in order to demonstrate the independence of its predictions from the specific adopted instrument.

To make available EMA4SM for everyone, we are considering the feasibility of hosting the software on public web site where users shall upload their measurements, and will download the predictions. At the same time manufacturers of portable reflectometers should be stimulated to make their instruments compliant with the concept of conic reflectance and capable to measuring conic-reflectance at least at five different values of acceptance angle in the range of interest; these data, together with the hemispherical reflectance measurement in the solar range, are sufficient to fit EMA4SM to any specific solar mirror for obtaining the exhaustive prediction of its solar-weighted features.

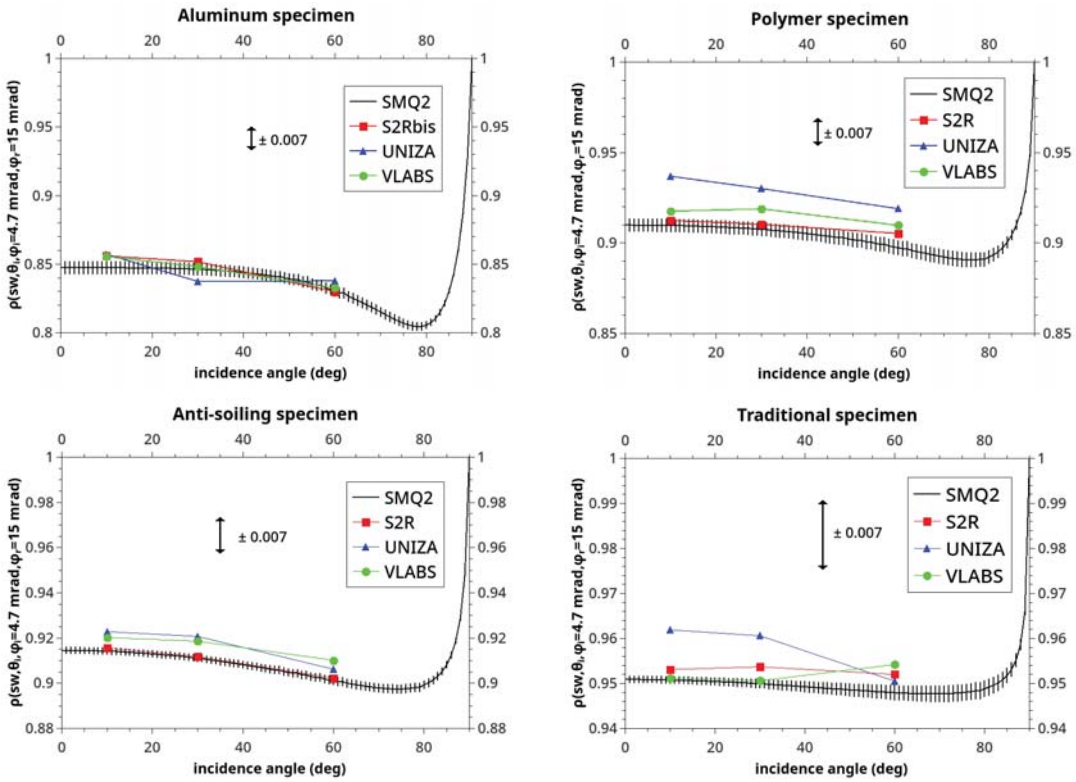

FIGURE 4. Comparison of EMA4SM predictions with experimental results got by several instruments at $\theta_i = 10,\ 30,\ 60$ deg and $\varphi = 15$ mrad on a specimen-set representative of the commercial production. The uncertainty of EMA4SM prediction represents the standard deviation among the evaluations achieved at the three wavelengths 480, 550, and 650 nm

Appendix: Computing SCR from Near-Specular Reflectance

Generally reflective coatings deposited on aluminium substrates diffuse radiation along one preferred direction, orthogonal to the specular axis, depending on the incidence angle and the orientation of the residual machining groves of the aluminium surface. This makes the scattering around the optical axis asymmetric. On the other hand, even in linear CSP systems, it is not possible to take advantage of such an asymmetry, because the asymmetry-direction depends on the incident angle. For this reason is commonly accepted to measure the amount of radiation reflected in a given φ as a whole, without analysing its asymmetry around the specular axis. For the same reason in the following SCR is evaluated by approximating the scattering distribution around the specular direction as symmetric.

Let Φ be the flux of the reflected solar-beam suitably normalised to return the hemispherical reflectance value when integrated over the half-space, thus

$$\rho_s(SW, \theta_i, \varphi) = \int_0^{2\pi} \int_0^{\varphi} \Phi(\theta_i, \alpha, \varphi')\, \varphi'\, d\alpha\, d\varphi' = 2\pi \int_0^{\varphi} \Phi(\theta_i, \varphi')\, \varphi'\, d\varphi' \tag{13}$$

where the radial symmetry around the specular axis is assumed. By computing the first derivative to φ of both terms of Equation 13, and with minor adjustments we have:

$$\Phi(\theta_i, \varphi) = \frac{1}{2\pi\varphi} \frac{\partial \rho_s(SW, \theta_i, \varphi)}{\partial \varphi} \tag{14}$$

where the right member can be numerically computed from the predictions of EMA4SM.

Equation 14 represents the behaviour of a low-divergent (plane wave) light beam reflected at a given point of the solar mirror. In order to evaluate the behaviour of the bundle of rays coming from the Sun, we have to consider the reflection of each one of those rays; summing up and averaging we obtain

$$\Phi_{sun}(\theta_i, \varphi) = \frac{1}{\Omega_{sun}} \int_{\Omega_{sun}} d\Omega \, \Phi(\theta_i, |\overrightarrow{\varphi} - \overrightarrow{\varphi_s}|) \tag{15}$$

where $\overrightarrow{\varphi_s}$ and $\overrightarrow{\varphi}$ are 2D vectors indicating the following angular displacements: from the point where $d\Omega$ is, to the Sun centre (the first) and from the diffuse ray to the specular axis (the second). Because we are only interested in the near-specular component, in the integration θ_i is a constant, set to the incidence angle formed by the axis of the cone containing the bundle of impinging solar rays and the normal to the mirror surface.

Finally SCR is obtained by integrating $\Phi_{sun}(\theta_i, \varphi)$ over the acceptance-angle of the receiver

$$SCR(\theta_i, \varphi) = 2\pi \int_0^{\varphi} \Phi_{sun}(\theta_i, \varphi') \, \varphi' \, d\varphi' \tag{16}$$

For $\varphi < 4.73$ mrad the behaviour of SCR greatly differs from that of $\rho_s(SW, \theta_i, \varphi)$. As an example

$$\lim_{\varphi \to 0} SCR(\theta_i, \varphi) = 0 \tag{17}$$

because SCR represents the solar radiation captured by the receiver, which becomes a point for $\varphi = 0$, and can not collect radiation. On the other hand

$$\lim_{\varphi \to 0} \rho_s(SW, \theta_i, \varphi) = \rho_s(SW, \theta_i, 0) > 0 \tag{18}$$

where $\rho_s(SW, \theta_i, 0)$ is the genuine specular solar reflectance related to the radiation travelling as a plane wave in the specular direction.

When $\varphi \geq 4.73$ mrad, the difference is much lower because the acceptance-angle of the receiver is large enough to avoid pure geometrical losses related to the Sun shape. When φ is large enough, $SCR(\theta_i, \varphi) \cong \rho_s(SW, \theta_i, \varphi)$.

ACKNOWLEDGMENTS

The development of EMA4SM as well as great part of the improvement of the instruments developed for measuring ner-specular and conic reflectance were supported by the SolarPACES project *Measuring and modelling near-specular solar reflectance at different incidence angle* in Task III, approved at the 92nd SolarPACES ExCo held in Thessaloniki, Greece, 4th April 2017. Moreover, we thank ENEA for providing access to its installations, the support of its scientific and technical staff, and the financial support of the SFERA-III project (Grant Agreement No 823802).

REFERENCES

[1] SolarPACES, *CSP - How it Works* (2016).
[2] A. Fernández-García, F. Sutter, M. Montecchi, F. Sallabery, A. Heimsath, C. Heras, E. Le Baron, and A. Soum-Glaude, *Parameters and Method to Evaluate the Reflectance Properties of Reflector Materials for Concentrating Solar Power Technology, V 3.0* (2018).
[3] S. Meyen, A. Fernandez, C. Kennedy, and E. Lüpfert, "Standardization of solar mirror reflectance measurements – round robin test," in *Proceedings of SolarPACES 2010* (2010).
[4] M. Montecchi, "Upgrading of enea solar mirror qualification set-up," in *Energy Procedia*, Vol. 49 (2014), pp. 2154–2161.
[5] M. Montecchi, Solar Energy **92**, 280–287 (2013).
[6] A. Heimsath, T. Schmid, and M. Nitz, P., Energy Procedia **69**, p. 1895–1899 (2015).
[7] F. Sutter, M. Montecchi, H. Von Dahlen, A. Fernández-García, and M. Röger, Solar Energy Materials and Solar Cells **176**, p. 119–133 (2018).
[8] M. Montecchi, "Proposal of a new parameter for the comprehensive qualification of solar mirrors for csp applications," in *AIP Conference Proceedings*, Vol. 1734 (2016).

[9] M. Montecchi, E. Nichelatti, and P. Polato, Solar Energy Materials and Solar Cells **71**, 327–342 (2002).
[10] ISO9050, *Glass in building, Determination of light transmittance, solar direct transmittance, total solar energy transmittance, ultraviolet transmittance and related glazing factors* (2003).
[11] L. Vriens and W. Rippens, Applied Optics **22**, 4105–4110 (1983).
[12] A. Beckman, P.and Spizzichino, *The scattering of electromagnetic waves from rough surfaces* (Pergamon/Macmillan, 1963).
[13] W. E. Born, M., *Principles of Optics* (1965).
[14] M. Montecchi, C. Delord, O. Raccurt, A. Disdier, F. Sallaberry, A. García de Jalón, A. Fernández-García, S. Meyen, C. Happich, A. Heimsath, and W. Platzer, Energy Procedia **69**, 1904–1910 (2015).
[15] E. Nichelatti, J. Opt. A: Pure Appl. Opt. **4**, 400–403 (2002).
[16] F. Sutter, A. Fernández-García, A. Heimsath, M. Montecchi, and C. Pelayo, "Advanced measurement techniques to characterize the near-specular reflectance of solar mirrors," in *AIP Conference Procedia*, Vol. 2126 (2019), pp. 2154–2161.